Modulation of Kv1.5 Potassium Channel Gating by Extracellular Zinc

Shetuan Zhang, Steven J. Kehl, and David Fedida
Department of Physiology, University of British Columbia, Vancouver, British Columbia V6T 1Z3, Canada

ABSTRACT Zinc ions are known to induce a variable depolarizing shift of the ionic current half-activation potential and substantially slow the activation kinetics of most K^+ channels. In Kv1.5, Zn^{2+} also reduces ionic current, and this is relieved by increasing the external K^+ or Cs^+ concentration. Here we have investigated the actions of Zn^{2+} on the gating currents of Kv1.5 channels expressed in HEK cells. Zn^{2+} shifted the midpoint of the charge-voltage (*Q-V*) curve substantially more (~2 times) than it shifted the $V_{1/2}$ of the *g-V* curve, and this amounted to +60 mV at 1 mM Zn^{2+}. Both Q1 and Q2 activation charge components were similarly affected by Zn^{2+}, which indicated free access of Zn^{2+} to channel closed states. The maximal charge movement was also reduced by 1 mM Zn^{2+} by ~15%, from 1.6 ± 0.5 to 1.4 ± 0.47 pC ($n = 4$). Addition of external K^+ or Cs^+, which relieved the Zn^{2+}-induced ionic current reduction, decreased the extent of the Zn^{2+}-induced *Q-V* shift. In 135 mM extracellular Cs^+, 200 μM Zn^{2+} reduced ionic current by only 8 ± 1%, compared with 71% reduction in 0 mM extracellular Cs^+, and caused a comparable shift in both the *g-V* and *Q-V* relations (17.9 ± 0.6 mV vs. 20.8 ± 2.1 mV, $n = 6$). Our results confirm the presence of two independent binding sites involved in the Zn^{2+} actions. Whereas binding to one site accounts for reduction of current and binding to the other site accounts for the gating shift in ionic current recordings, both sites contribute to the Zn^{2+}-induced *Q-V* shift.

INTRODUCTION

Divalent metal cations are well known to modify the gating of ion channels (Frankenhaeuser and Hodgkin, 1957; Gilly and Armstrong, 1982b; Spires and Begenisich, 1990; Davidson and Kehl, 1995), and sometimes this action results in equal shifts in the voltage-dependent kinetics of Na^+ and K^+ channels. As a result, surface charge effects are often invoked to explain many of the actions (Hille, 1992; Elinder et al., 1996). The block of Na^+ and K^+ channels by polyvalent ions like Zn^{2+} has a number of characteristics that suggest specific binding to the channel rather than a general action related to surface charge screening. The first is the potency of Zn^{2+} action. Zn^{2+} can cause a 70-mV shift in the *g-V* relation at micromolar concentrations, whereas other divalent cations like Ca^{2+} and Mg^{2+} rarely achieve an equivalent effect (Spires and Begenisich, 1994; Elinder et al., 1996). Zn^{2+} also has quite different effects on the activation and deactivation gating of channels. In the squid axon, external Zn^{2+} substantially slows Na^+ and K^+ current activation (Gilly and Armstrong, 1982b; Spires and Begenisich, 1992) while having much less effect on channel deactivation kinetics (Gilly and Armstrong, 1982a). These findings have been explained by the presence of a Zn^{2+} receptor site accessible during the resting state and which disappears in the open state due to the conformational changes of the channel upon opening (Gilly and Armstrong, 1982a). Clearly, this is an expression of state-dependent binding to the channel, and the idea has been complemented by a recent study showing fast and selective Zn^{2+} binding to resting neuronal K^+ channels (Kuo and Chen, 1999).

A more complete understanding of Zn^{2+} action on channel states that do not report conformational changes by altering ion flux requires measurements of gating currents recorded as channels proceed through closed states in the activation pathway. Earlier gating current studies are consistent with the ionic current data and showed that external Zn^{2+} slowed the on-gating currents of squid axon Na^+ channels, while having little effect on off-gating current (Gilly and Armstrong, 1982b). However, more recently, both internal and external Zn^{2+} have been shown to cause only modest changes in squid axon K^+ channel gating currents in a limited range of potentials near −30 mV (Spires and Begenisich, 1995). Based on these observations, it has been proposed that Zn^{2+} modifies conformational changes of the squid K^+ channels that are only weakly voltage dependent, most likely occurring toward the final opening transition.

In the cloned Kv1.5 channel we have recently shown that in addition to a Zn^{2+}-induced depolarizing shift of the channel half-activation potential ($V_{1/2}$), and substantial slowing of channel activation, Zn^{2+} causes a concentration-dependent reduction of Kv1.5 current (Zhang et al., 2001). Increasing external K^+ or addition of Cs^+ relieves this reduction but has little effect on the gating shift, and we have proposed at least two binding sites for Zn^{2+}. To clarify conflicting studies of the actions of Zn^{2+} on channel states within the activation pathway, here we have directly studied the effects of external Zn^{2+} on ionic and gating currents of Kv1.5 channels. This allows us to address the influence of external Zn^{2+} on the activation charge movement in Kv1.5 channels. Unlike any other reported channels, Zn^{2+} causes a substantial depolarizing shift of the midpoint of the charge-voltage (*Q-V*) curve, which is larger than the Zn^{2+}-

Received for publication 18 January 2001 and in final form 2 April 2001.
Address reprint requests to Dr. David Fedida, Department of Physiology, University of British Columbia, 2146 Health Sciences Mall, Vancouver B.C. V6T 1Z3, Canada. Tel.: 604-822-5806; Fax: 604-822-6048; E-mail: fedida@interchange.ubc.ca.

0006-3495/01/07/125/12 $2.00

induced shift of the conductance-voltage (*g-V*) relation. Addition of external K^+ or Cs^+, which relieves Zn^{2+}-induced ionic current reduction, decreases the extent of the Zn^{2+}-induced *Q-V* shift. Our experiments suggest that there are two components to the depolarizing shift of the activation of Kv1.5 channels as recorded by gating currents. The first involves Zn^{2+} binding to a site or sites in Kv1.5 channels that displaces gating to more positive potentials and has the macroscopic effect of slowing Kv1.5 ionic current activation. It appears that the channel is accessible to Zn^{2+} binding at a number of states within the activation pathway. The second component of the gating charge displacement appears coupled to the blocking action of Zn^{2+}.

MATERIALS AND METHODS

Cells and solutions

Kv1.5 currents were recorded from channels expressed in a human embryonic cell line (HEK293) using LipofectACE reagent (Canadian Life Technologies, Bramalea, Ontario, Canada). The Kv1.5 cDNA subcloned into pRc/CMV was transfected into HEK293 cells. These were maintained in minimum essential medium, 10% fetal bovine serum, penicillin-streptomycin and G418 (0.5 mg/ml) to select for transfected cells. Patch pipettes contained (in mM): 135 KCl, 5 EGTA, 10 HEPES, 1 $MgCl_2$, 4 Na_2ATP, and 0.1 GTP. pH was adjusted to 7.2 with KOH. The bath solution contained (in mM): 135 NaCl, 5 KCl, 10 HEPES, 1 $MgCl_2$, and 2 $CaCl_2$. The pH was adjusted to 7.4 with NaOH. For 135 mM Cs^+-containing solution, CsCl replaced KCl.

To record gating currents, an HEK cell line stably expressing Kv1.5-W472F mutant channels was used. This mutation is analogous to the ShH4-IR W434F mutation, which abolishes K^+ conduction in *Shaker* channels (Perozo et al., 1993). Patch pipettes contained (in mM): 140 *N*-methyl-D-glutamine (NMG), 1 $MgCl_2$, 10 HEPES, and 10 EGTA, adjusted to pH 7.2 with HCl. The standard bath solution contained (in mM): 140 NMG, 1 $MgCl_2$, 10 HEPES, 2 $CaCl_2$, and 10 glucose. pH was adjusted to 7.4 with HCl. For 135 mM Cs^+-containing solution, CsCl replaced NMG. For 5 mM K^+-containing solution, 5 mM KCl was added to the standard solution and NMG proportionally reduced. In three gating current experiments, extracellular NMG was replaced by 135 mM NaCl, and no difference was found in the magnitude of the gating shift compared with when NMG alone was used. All chemicals were from Sigma Aldrich Chemical Co. (Mississauga, Ontario, Canada). We could not increase extracellular K^+ concentration further than 5 mM in the gating current recordings because inward K^+ ionic current through endogenous channels contaminated the gating currents.

Electrophysiological procedures

Coverslips containing cells were removed from the incubator before experiments and placed in a superfusion chamber containing the control bath solution at 22–23°C. The bath solution was constantly flowing through the chamber, and the solution was exchanged by switching the perfusates at the inlet of the chamber, with complete bath solution changes taking 1–2 s. Whole-cell current recording and data analysis were done using an Axopatch 200A amplifier and pClamp6 software (Axon Instruments, Foster City, CA). Patch electrodes were fabricated using thin-walled borosilicate glass (World Precision Instruments, Sarasota, FL). The electrodes had resistances of ~2 MΩ for ionic current recordings and between 1 and 2 MΩ for gating current recording. Capacitance compensation was routinely used. Data were filtered at 10 kHz and sampled at 50 kHz for all protocols. Series resistance (R_s) compensation was used in recording ionic K^+ currents but was not used in gating current recordings due to their relatively small size. Leak subtraction was not used in the ionic current recordings but routinely used in the gating current recordings where leakage and capacitive currents were subtracted on-line using a P/6 protocol. Data are shown as mean ± SE.

RESULTS

Effects of extracellular Zn^{2+} on Kv1.5 ionic currents

Data in Fig. 1 illustrate the effects of extracellular application of 1 mM Zn^{2+} on Kv1.5 ionic current. The protocol shown above Fig. 1 *A* was used to study Zn^{2+} effects on activation properties of the channel in a voltage range between −60 mV and 80 mV. Fig. 1 *A* shows superimposed currents elicited in control conditions, and Fig. 1 *B* shows currents in the presence of Zn^{2+} at a concentration of 1 mM. Zn^{2+} significantly slowed the channel activation and decreased current amplitude. A second protocol shown above Fig. 1 *C* was used to study Zn^{2+} effects on deactivation properties in a voltage range between +10 and −70 mV after a depolarizing step to +50 mV to activate the channel. Compared with control (Fig. 1 *C*), 1 mM Zn^{2+} caused a moderate acceleration of the current decay upon repolarization (Fig. 1 *D*). Quantitative analyses of Zn^{2+} effects on Kv1.5 channel kinetics are illustrated in Fig. 1, *E* and *F*. Normalized activation curves with the activation curve before normalization in the inset are shown in Fig. 1 *E* where 1 mM Zn^{2+} shifted the midpoint of the activation curve by 33 mV in the depolarized direction and decreased the maximal conductance by 67%. Fig. 1 *F* shows activation and deactivation time constants at different membrane potentials. τ_{act} was determined by a single exponential fit to the current activation between 10% and 90% of the maximal current (data in Fig. 1, *A* and *B*). The values obtained at potentials ≥−10 mV in control (△) and ≥+20 mV in the presence of Zn^{2+} (▲) are activation time constants. τ_{deac} was obtained by single exponential fit to the tail current decay at potentials ≤−20 mV in control (▽) and ≤+10 mV in the presence of Zn^{2+} (▼) from data in Fig. 1, *C* and *D*. Zn^{2+} decreased the deactivation time constant and increased the activation time constant. The effects of Zn^{2+} on Kv1.5 channels were totally reversible (data not shown). As noted previously in other K^+ channels (Gilly and Armstrong 1982; Spires and Begenisich, 1992, 1994), the effects on the deactivation time constant were small and equivalent to a shift of ~+20 mV. In contrast, the effects on the activation time constant were large and equivalent to a shift of ~+50 mV. Therefore, the effects of Zn^{2+} on the time constants cannot be explained by a simple shift along the potential axis. To understand the actions of Zn^{2+} during activation and the rate-limiting step of deactivation, we have measured gating currents from Kv1.5.

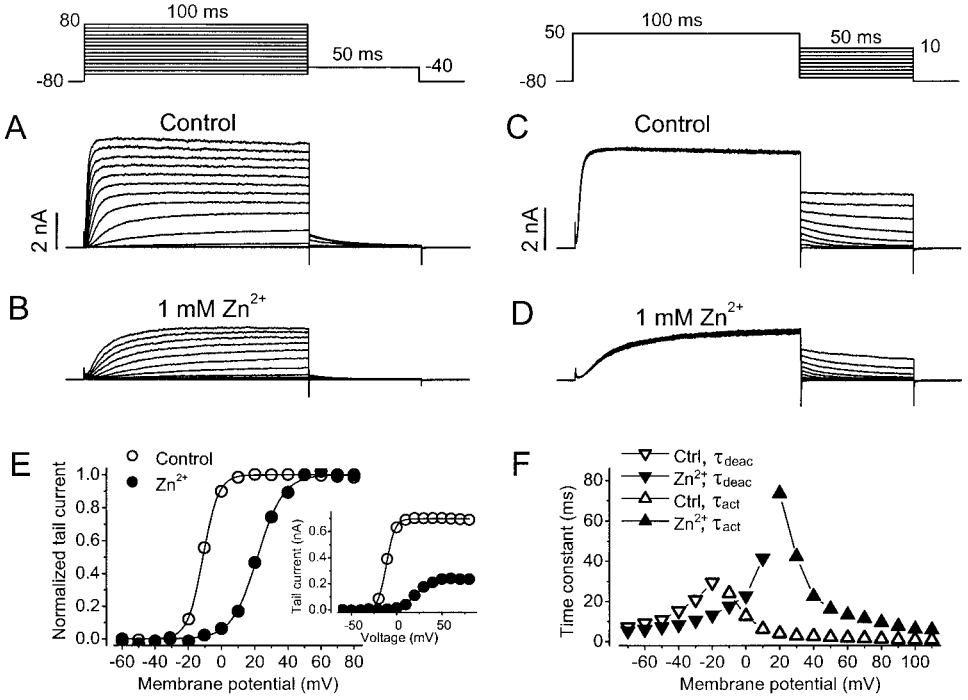

FIGURE 1 The effects of extracellular Zn^{2+} on Kv1.5 ionic currents expressed in HEK cells. The two protocols used to elicit Kv1.5 current are shown above the current traces in *A* and *C*. In *A* (control) and *B* (1 mM Zn^{2+}), cells were held at −80 mV and pulsed to between −60 and +80 mV for 100 ms before returning to −40 mV to record deactivating tail currents. In *C* (control) and *D* (1 mM Zn^{2+}), cells were pulsed to +50 mV from the holding potential of −80 mV for 100 ms before returning to a range of potentials between +10 and −70 mV to record tail currents. (*E*) Normalized activation curves obtained by plotting the peak of the tail current from data in *A* and *B* relative to its maximal value against the pulse voltages in control (○) and 1 mM Zn^{2+} (●). $V_{1/2}$ and *k*, respectively, were −11.6 and 4.5 mV in control and +21.9 and 7.8 mV in the presence of 1 mM Zn^{2+}. The activation curves before normalization are shown in the inset of *E* where the current reduction is also obvious. (*F*) Activation (△) and deactivation (▽) time constants in control and in the presence of 1 mM Zn^{2+} (▲, ▼). Activation time constants were obtained by single exponential fitting to the rising phase of the current upon depolarization from *A* and *B*, and the deactivation time constant was obtained from the tail current decays in *C* and *D*.

Effects of extracellular Zn^{2+} on Kv1.5 channel gating currents

Stable expression of the nonconducting mutant Kv1.5-W472F (NCM) in HEK293 cells allowed the recording of large gating currents with good time resolution. Gating currents from this mutated channel are very similar to those observed with the wild-type Kv1.5 channel (Hesketh and Fedida, 1999). Examples of gating current traces in the absence and presence of 1 mM Zn^{2+} are presented in Fig. 2, *A* and *B*, from one cell. In control conditions, on-gating currents appeared upon depolarizations positive to −60 mV. As depolarizing steps became stronger, on-gating current increased in amplitude and decayed more rapidly. Off-gating currents upon repolarization to −100 mV have a rapid decay time course after small depolarizations up to 0 mV. After more positive depolarizations, off-gating currents at −100 mV decreased in amplitude and decayed more slowly. The reasons for the slowing likely include the reversal of a relatively voltage-independent rearrangement that occurs on pore opening and rapid onset inactivation that is also slow to reverse (Zagotta et al., 1994; Ledwell and Aldrich, 1999; Chen et al., 1997). Fig. 2 *B* illustrates the action of 1 mM Zn^{2+} on the gating current. For identical voltage pulses, the currents in the presence of Zn^{2+} are reduced, mostly due to a substantial shift of the voltage dependence. At more positive potentials, the peak amplitudes of currents in the presence of Zn^{2+} approach those in the control conditions. Although Zn^{2+} reduced the total charge movement by only ~15% (see Table 1) with maximal depolarization, a +60-mV shift was apparent in the charge-voltage (*Q-V*) relationship (Fig. 2 *C*). Zn^{2+} also accelerated the charge return upon repolarization to −100 mV (Fig. 2 *B*). The effects of Zn^{2+} on charge return are considered in greater detail below (see Fig. 9).

To quantify the Zn^{2+} effects on gating current, the amount of charge moved upon depolarization was determined by integrating the on-gating current. The data in the absence and presence of Zn^{2+} were normalized to the maximum charge moved in the absence of Zn^{2+}. The relationship between on-gating charge and membrane potential in the absence and presence of 1 mM Zn^{2+} are shown in Fig. 2, *C* and *D*. As we reported previously, the amplitude of Q_{on} at different depolarizing potentials (*Q-V* curve) reveals a relationship with strong sigmoidicity (Hesketh and

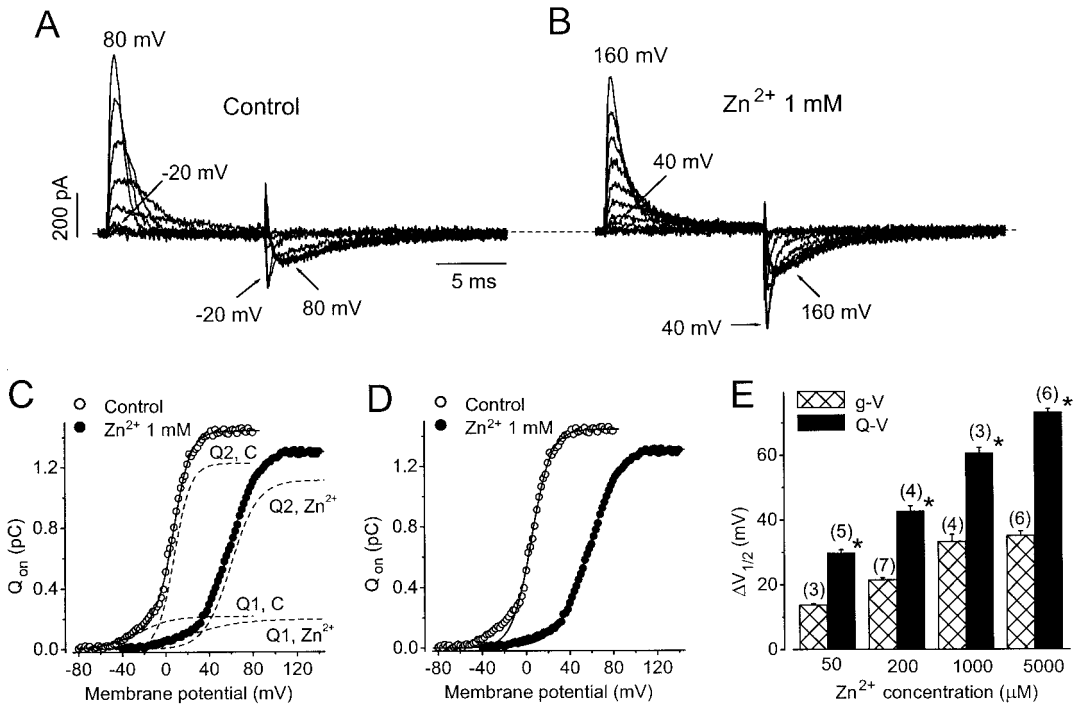

FIGURE 2 Effects of extracellular Zn^{2+} on Kv1.5 channel gating currents. (*A* and *B*) Gating currents in the absence (*A*) and in the presence (*B*) of 1 mM Zn^{2+}. In control conditions, cells were depolarized from −100 mV to between −80 and 80 mV in 2-mV increments for 12 ms. In 1 mM Zn^{2+}, cells were depolarized to between −40 and 160 mV in 2-mV increments. Traces shown in *A* and *B* are in increments of 20 mV. (*C*) Amount of charge moved upon depolarization (Q_{on}) was determined by integrating the on-gating current in control (○) and 1 mM Zn^{2+} (●). The solid lines are fits of data to a double Boltzmann equation. (*D*) Fits of the *Q-V* relations with a single Boltzmann function. $V_{1/2}$ and *k*, respectively, were −1 and 6 mV in control, and +60 and 15 mV in the presence of 1 mM Zn^{2+}. Zn^{2+} also reduced Q_{max} by 10%. (*E*) Concentration dependence of Zn^{2+}-induced $V_{1/2}$ shifts in *Q-V* (*solid bars*) and *g-V* (*hatched bars*) curves. Zn^{2+}-induced shifts of the *Q-V* relations were greater than those of the *g-V* relations at all Zn^{2+} concentrations. *$p < 0.05$.

Fedida, 1999). A single Boltzmann function fit to the relation was not satisfactory (Fig. 2 *D*) because of the shallow rising phase of the curve (the foot) and the steeper voltage dependence of charge movement at higher voltages. This suggested a component of the overall gating charge with a shallower voltage dependence activated at lower depolarizations and a second more voltage-dependent component activated at more depolarized voltages. The data points were fit with a double Boltzmann function (Fig. 2 *C*), and the component single Boltzmann functions were then plotted on the same axes and termed Q1 and Q2. Q1 is the smaller component, is less voltage dependent, and is activated at lesser depolarizations than the Q2 component. Results shown in Table 1 indicate that Zn^{2+} greatly shifted the voltage-dependent parameters of both Q1 and Q2 in Kv1.5 channels. Zn^{2+} shifted the $V_{1/2}$ for both Q1 and Q2 between +50 and +60 mV along the potential axis. In addition, there was a significant decrease of the voltage sensitivity both of Q1 and Q2 in the presence of Zn^{2+}.

Of interest in the present study was the finding that Zn^{2+} shifted the *Q-V* relation (Fig. 2 *C*) far more than the *g-V* relationship (Fig. 1 *E*). To quantify the Zn^{2+}-induced shift, we fitted the *Q-V* relations with a single Boltzmann function to judge the Zn^{2+}-induced shift of the overall relationship (Fig. 2 *D*). This seemed reasonable as Q2, which is more directly related to channel opening, dominates the *Q-V* relation and accounts for more than 80% of total charge movement. Also, Zn^{2+} similarly affected Q1 and Q2 (Table

TABLE 1 Effect of Zn^{2+} on parameters of the double-Boltzmann fit to the *Q-V* curves summarized from six cells

	Q_{1max} (fC)	V_1 (mV)	k_1 (mV)	Q_{2max} (fC)	V_2 (mV)	k_2 (mV)
Control	245 ± 76	−25.3 ± 2.7	12.5 ± 1.2	1388 ± 438	+4.6 ± 1.0	5.9 ± 0.6
1 mM Zn^{2+}	213 ± 69	+29.2 ± 39*	22.2 ± 1.9*	1222 ± 402	+62.4 ± 1.5*	13.1 ± 0.9*

Q_{1max} and Q_{2max}, maximum on-gating charges of Q_1 and Q_2, respectively; V_1 and V_2, half activation potentials for Q_1 and Q_2, respectively; k_1 and k_2, steepness of voltage dependence of Q_1 and Q_2, respectively.

*$p < 0.01$. The total charge (Q1 + Q2) was significantly reduced from 1.6 ± 0.51 pC in control to 1.4 ± 0.47 pC in the presence of 1 mM Zn^{2+} (paired *t*-test, $n = 4$, $p < 0.05$).

1). The Zn^{2+}-induced shift of the midpoint of the *Q-V* curve was concentration dependent (Fig. 2 *E*). As noted above, the Zn^{2+}-induced *Q-V* shifts are significantly larger than the Zn^{2+}-induced *g-V* shift at all concentrations tested, as summarized in Fig. 2 *E*.

The effect of Zn^{2+} on Q2 is not dependent on an effect on Q1

We have shown that Zn^{2+} similarly affects the voltage sensitivity of both Q1 and Q2. Multiple charge systems in *Shaker* channels (Bezanilla et al., 1994) and Kv1.5 (Hesketh and Fedida, 1999) generally show sequentiality so that there are two possibilities for the Zn^{2+}-induced shift of Q2 charge movement. One possibility is that Zn^{2+} directly affects Q2 charge, and the second possibility is that Zn^{2+} affects Q2 as a consequence of its action on Q1. This arises because Q2 can move only after Q1 according to a sequential model of gating. The experiments in Figs. 3 and 4 were designed to discriminate between these possibilities.

There is a 30-mV difference between the half-activation potentials of Q1 and Q2 (V1 and V2, Table 1). This difference enables us to separate the two charge systems. Very little Q2 moves at voltages negative to −20 mV (Fig. 2 *C*), so gating current elicited by depolarizing pulses to −20 mV should move Q1 almost exclusively. In addition, after a prepulse to −20 mV, which moves almost all of Q1, gating currents during test pulses to more depolarized potentials should reflect largely Q2 movement. Fig. 3 *A* shows control current during a prepulse to −20 mV and subsequently during a depolarization to +100 mV. The current during the prepulse reflects Q1, and a larger transient current reflects Q2 upon subsequent depolarization to +100 mV. In the presence of 1 mM Zn^{2+} and using the same voltage protocol, Q1 was not moved by the prepulse, and Q1 + Q2 movement was slowed in the presence of Zn^{2+} during the test pulse (Fig. 3 *B*). In Fig. 3 *C* in the presence of Zn^{2+}, the prepulse potential was increased to +20 mV to force Q1 to move. Nevertheless, upon subsequent depolarization to +100 mV, Q2 movement was still slowed by Zn^{2+}. The time courses of charge movement in Fig. 3, *A–C*, are shown in Fig. 3 *D*. It can be seen that Q2 charge movement is always slower in the presence of Zn^{2+}, whether or not Q1 is moved. These results suggested that Zn^{2+} effects on Q2 were not directly as a result of Zn^{2+}-induced slowing of prior Q1 movement but that in both cases Q2 movement was affected by prior exposure of Q1 channel states to Zn^{2+}.

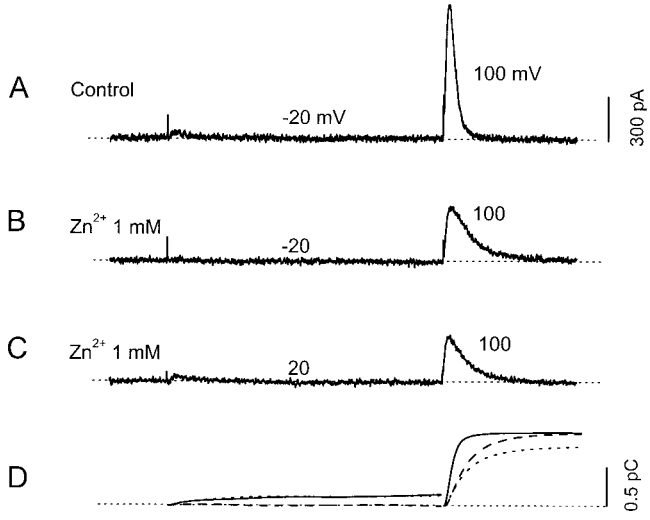

FIGURE 3 Both Q1 and Q2 movement was affected by external Zn^{2+}. (*A* and *B*) Gating current was recorded from −100 mV to −20 mV for 24 ms to activate Q1, followed by a depolarizing pulse to +100 mV to move Q2 in control (*A*) and in 1 mM Zn^{2+} (*B*). (*C*) In 1 mM Zn^{2+}, a prepulse to +20 mV forced Q1 movement before a pulse to +100 mV to move Q2. Movement of Q1 had no effect on Zn^{2+}-induced slowing of Q2 movement. (*D*) Superimposed Q_{on} from *A* (——), *B* (– – –), and *C* (· · ·).

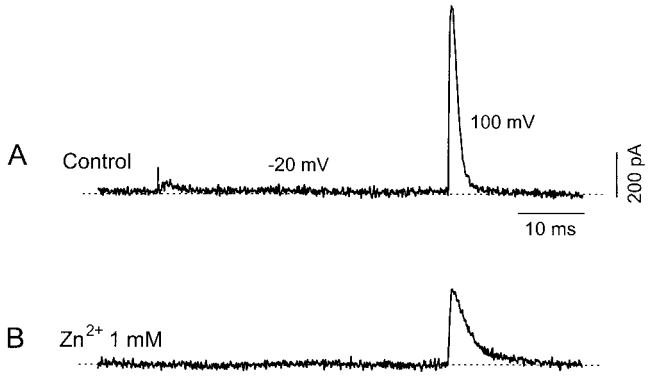

FIGURE 4 Q2 movement is affected by Zn^{2+} addition after Q1 movement. (*A*) Control gating current was recorded from −100 mV to −20 mV for 24 ms to activate Q1, followed by a depolarizing pulse to +100 mV to move Q2. (*B*) 1 mM Zn^{2+} was washed in after Q1 movement by the prepulse to −20 mV. Q2 movement was slowed during a pulse to +100 mV in the presence of 1 mM Zn^{2+}.

We attempted to prevent prior exposure of Q1 states to Zn^{2+} in the experiment illustrated in Fig. 4. Here using the same protocol as in Fig. 3, after the control double pulse recording (Fig. 4 *A*), the potential was held at −20 mV to move Q1 and the cell exposed to 1 mM extracellular Zn^{2+}. In this situation, Q2 movement is still slowed (Fig. 4 *B*), which indicates the ability of Zn^{2+} to bind to and influence later channel states and charge movement beyond Q1 in the activation pathway.

Increasing K_o^+ reduces the Zn^{2+}-induced *Q-V* shift

Previously, we have demonstrated that Zn^{2+} reduction of Kv1.5 ionic current is strongest in the absence of external K^+ (Zhang et al., 2001). Raising the external K^+ or Cs^+ concentrations relieved the Zn^{2+} block but did not affect the

Zn^{2+}-induced *g-V* shift. Based on these observations we suggested that the Zn^{2+}-induced *g-V* shift and current reduction may involve two independent binding sites. Here we have found that the Zn^{2+} -induced shift of the *Q-V* is greater than that of the *g-V*, so we hypothesized that this extra voltage-dependent shift of the *Q-V* was related to Zn^{2+} binding to the blocking site. These blocked channels will not contribute to visible ionic current, so they cannot influence the position of the *g-V* relation, but gating charge may still move freely in these channels, and this may explain the greater depolarizing shift of the *Q-V* relation. The experiments in Figs. 5–8 tested whether raising K^+ or Cs^+ can relieve part of the *Q-V* shift.

With 0 mM K^+ in the external solution, on-gating currents in the presence of 1 mM Zn^{2+} were slowed compared with controls and reduced in amplitude even at +120 mV (Fig. 5, *A* and *B*). This corresponded to a shift in the *Q-V* curve of +61 mV (Fig. 5 *C*) and is consistent with the results shown in Fig. 2 *E*. When the external solution contained 5 mM K_o^+, gating currents at positive potentials were larger and decayed faster compared with 0 mM K_o^+. This is clearly seen by comparison of the +120-mV records in Fig. 5, *B* and *E*. In this situation, 1 mM Zn^{2+} shifted the *Q-V* curve by +49 mV (Fig. 5 *F*), a value significantly smaller ($p < 0.05$) than with external solution containing 0 mM K^+. The chart in Fig. 6 shows a quantitative comparison of the modulating effect of 0 mM and 5 mM K_o^+ on the ionic current reduction and the voltage-dependent shifts in the half-activation potentials of the *Q-V* and *g-V* curves caused by 50 μM and 1 mM Zn^{2+}. As we have shown previously (Zhang et al., 2001), 5 mM K_o^+ significantly decreased Zn^{2+}-induced block of ionic current. This concentration of K_o^+ also decreased the Zn^{2+}-induced *Q-V* shift from 30.2 ± 0.9 to 18.7 ± 0.9 mV and from 63.5 ± 1.1 to 50.7 ± 2.1 mV in 50 μM and 1 mM Zn^{2+}, respectively. The shift of the *g-V* relation, which was unaltered by changes in K_o^+ is shown as the broken lines for comparison. At 50 μM Zn^{2+} and 5 mM K_o^+, with minimal ionic current reduction

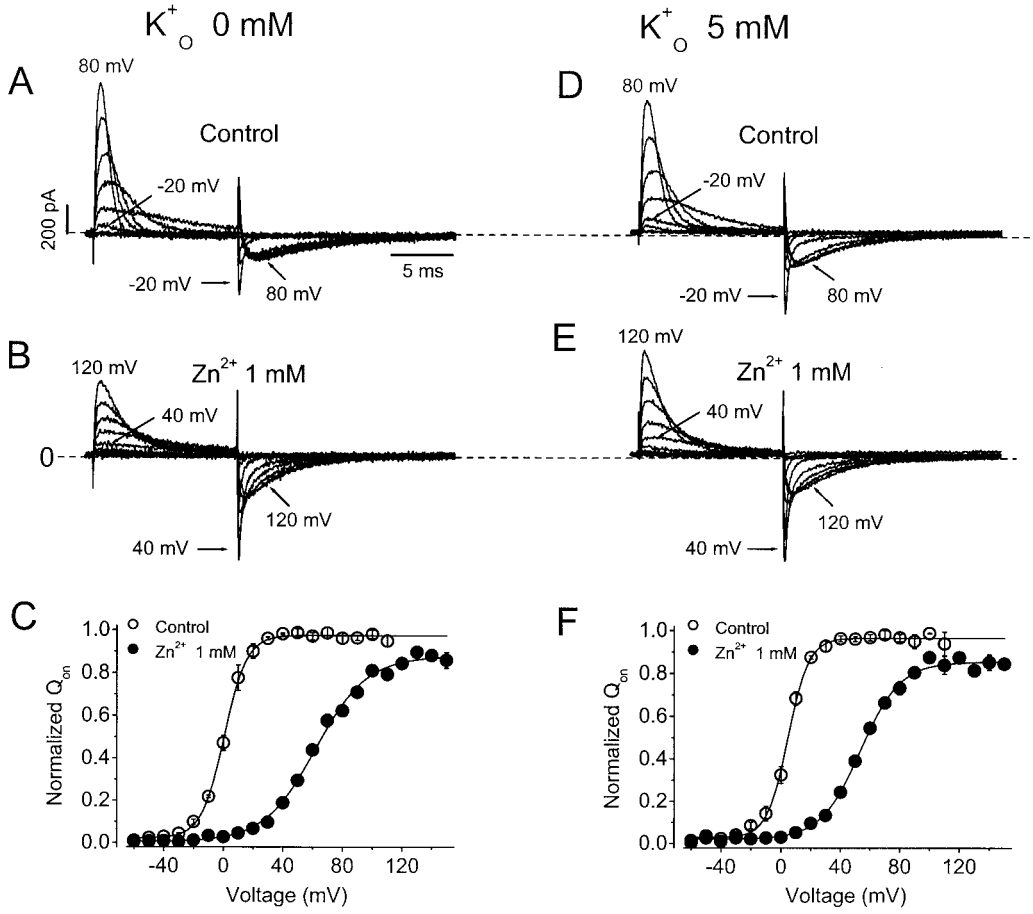

FIGURE 5 Increasing K_o^+ from 0 to 5 mM reduced the Zn^{2+}-induced *Q-V* shift. (*A*, *B*, *D*, and *E*) Gating currents recorded from two cells in 0 and 5 mM K_o^+, in control and the presence of 1 mM Zn^{2+}. Currents were recorded from −100 to between −60 and +90 mV (control) or +120 mV (Zn^{2+}) in 10-mV steps (data at 20-mV intervals are shown). (*C* and *F*) *Q-V* curves in control and 1 mM Zn^{2+} in 0 and 5 mM K_o^+, respectively. (*C*) $V_{1/2}$ and *k* were 0 and +7.8 mV in control and +60 and 15.2 mV, respectively, in 1 mM Zn^{2+} ($n = 6$). (*F*) Control $V_{1/2}$ and *k* were +5 and 7.8 mV, respectively, and then shifted to +50 and 15.2 mV in 1 mM Zn^{2+} ($n = 7$).

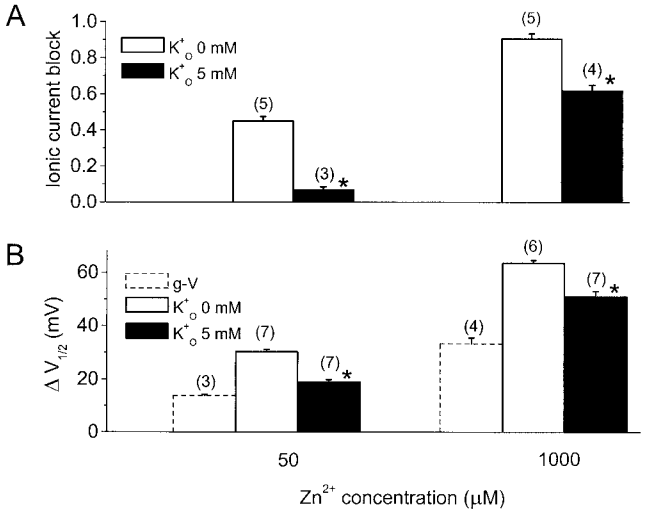

FIGURE 6 Relief of Zn^{2+}-induced ionic current reduction and *Q-V* shift by 5 mM K^+_o. (*A*) Relative ionic current reduction by 50 μM and 1 mM Zn^{2+} in 0 and 5 mM K^+_o. Block was 45% in 0 mM K^+_o and 7% in 5 mM K^+_o with 50 μM Zn^{2+}; with 1 mM Zn^{2+} it was 91% in 0 mM K^+_o and 62% in 5 mM K^+_o. (*B*) *Q-V* shift induced by 50 μM and 1 mM Zn^{2+} in 0 and 5 mM K^+_o. Addition of 5 mM K^+ to the external solution relieved Zn^{2+}-induced current reduction and it also reduced the Zn^{2+}-induced *Q-V* shift. $*p < 0.05$ compared with data in 0 mM K^+; number of cells tested is indicated in the parentheses above each bar.

there was no significant difference between the *g-V* and *Q-V* shifts (Fig. 5 *B*). However, at 1 mM Zn^{2+} the >50% reduction in 5 mM K^+_o was associated with a significantly greater shift of the *Q-V* than of the *g-V*.

Relief of Zn^{2+}-induced gating *Q-V* shift by 135 mM Cs^+

Cs^+ also partially relieves Zn^{2+} reduction of ionic current (Zhang et al., 2001) and the Cs^+ conductance of endogenous channels in HEK cells is negligible, so we compared the Zn^{2+}-induced shifts of the *g-V* and *Q-V* curves in 135 mM Cs^+-containing external solutions (Fig. 7). Ionic and gating currents under these conditions are shown in Fig. 7, *A* and *D*, in control and Fig. 7, *B* and *E*, in the presence of 200 μM Zn^{2+}. In this situation, 200 μM Zn^{2+} caused comparable shifts of the *g-V* and *Q-V* relations and similar changes in slope (Fig. 7, *C* and *F*). Data obtained from 5–8 cells are summarized in Fig. 8. The action of Cs^+ was to limit ionic current reduction by 200 μM Zn^{2+} to only 8% of control (Fig. 8 *A*) vs. 71 ± 2% ($n = 10$) in 0 mM Cs^+. In this situation, the *g-V* and *Q-V* shifts were comparable at 17.9 ± 0.6 and 20.8 ± 2.1 mV, respectively (Fig. 8 *B*). When the Zn^{2+} concentration was increased to 1 mM, the ionic current was reduced by 27%, and Zn^{2+} caused a significantly larger shift of the *Q-V* than the *g-V* relation (48.6 ± 1.6 mV vs. 31.0 ± 1.7 mV). Thus, it appears that the blocking effect is itself correlated with a partial shift of the *Q-V* relation.

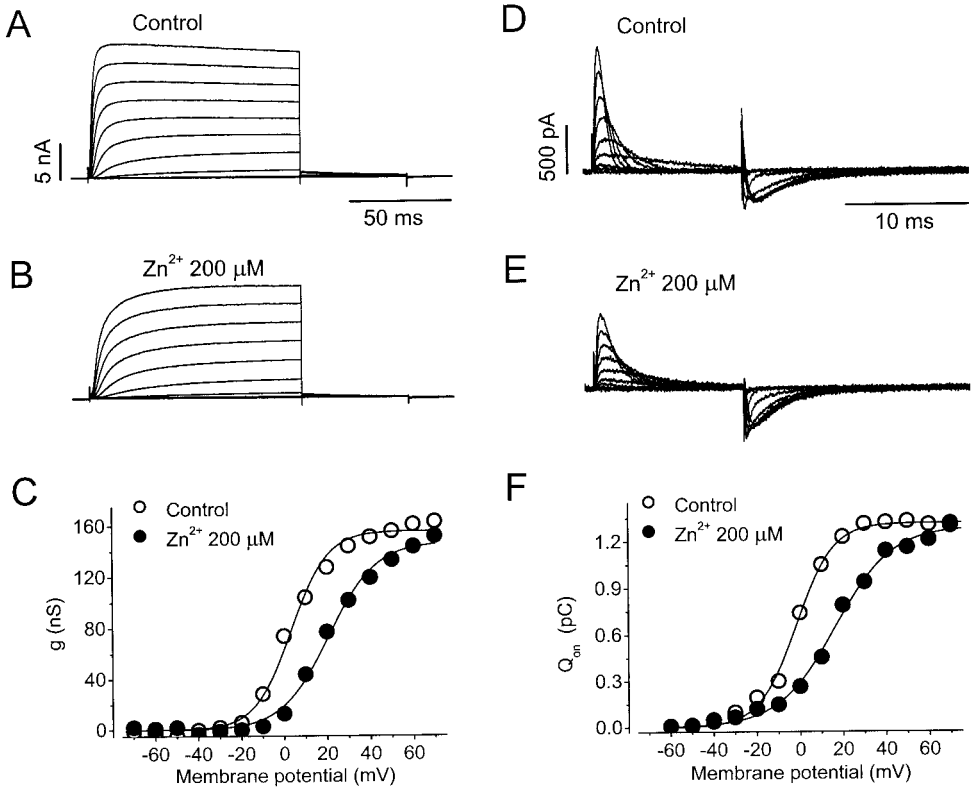

FIGURE 7 Zn^{2+}-induced *g-V* shift and *Q-V* shift are comparable in 135 mM Cs^+_o-containing external solutions. (*A* and *B*) Ionic currents in 135 mM Cs^+_o during depolarizations from −70 to +70 mV in 10-mV steps in control (*A*) and in 200 μM Zn^{2+} (*B*). (*C*) *g-V* curves from *A* and *B*. (*D* and *E*) Gating currents in 135 mM Cs^+_o from −60 mV to +100 mV (+120 mV in Zn^{2+}) in control (*D*) and in the presence of 200 μM Zn^{2+} (*E*). (*F*) *Q-V* curves from *D* and *E*; 200 μM Zn^{2+} caused a comparable shift of $V_{1/2}$ in *g-V* and *Q-V* curves. The $V_{1/2}$ and *k* of the *g-V* were +3.7 and 9.8 mV in control and +20.8 and 11.9 mV in 200 μM Zn^{2+}, respectively. The $V_{1/2}$ and *k* of the *Q-V* were −1.7 and 8.6 mV in control and +16.3 and 13.3 mV in 200 μM Zn^{2+}.

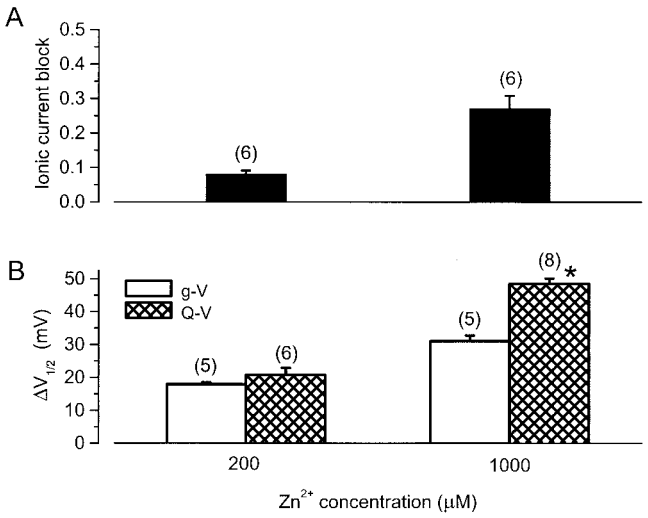

FIGURE 8 Reduction in Zn^{2+}-induced ionic current block and *Q-V* shift in 135 mM Cs_o^+. (*A*) Fraction of ionic reduction caused by 200 μM and 1 mM Zn^{2+} in 135 mM Cs_o^+ was 0.08 ± 0.01 and 0.27 ± 0.04, respectively ($n = 6$ cells). (*B*) Comparison of *Q-V* and *g-V* shifts induced by 200 and 1000 μM Zn^{2+} in 135 mM Cs_o^+. Note that at the higher Zn^{2+} concentration the *Q-V* shift was still significantly greater than the *g-V* shift; $*p < 0.05$.

External Zn^{2+} speeds gating charge return of Kv1.5 channels

When cells are repolarized to −100 mV, off-gating currents represent the return of gating elements as channels deactivate. It can be seen from data in Fig. 2 *B* that Zn^{2+} slightly accelerates the off-gating charge return upon repolarization. In Fig. 9, *A* and *B* (1 mM Zn^{2+}), charge return is shown as the downward current deflections after 12-ms depolarizations to between −60 and +120 mV. In control conditions (Fig. 9 *A*), for small depolarizations such as to −20 mV, off-gating currents reached a peak very rapidly and decayed rapidly. Following depolarizations to more positive potentials, the peak off-gating current was reduced, the time to peak was increased, and decay was dramatically slowed. Zn^{2+} shifted the voltage dependence of gating charge movement as described earlier, increased off-gating current amplitude, and speeded its decay (Fig. 9 *B*). Charge movements derived by time integration of records in Fig. 9, *A* and *B*, are shown in Fig. 9, *C* and *D*. The on-gating charge waveforms reflect the time- and voltage-dependent movement of gating charge as channels progress toward the open

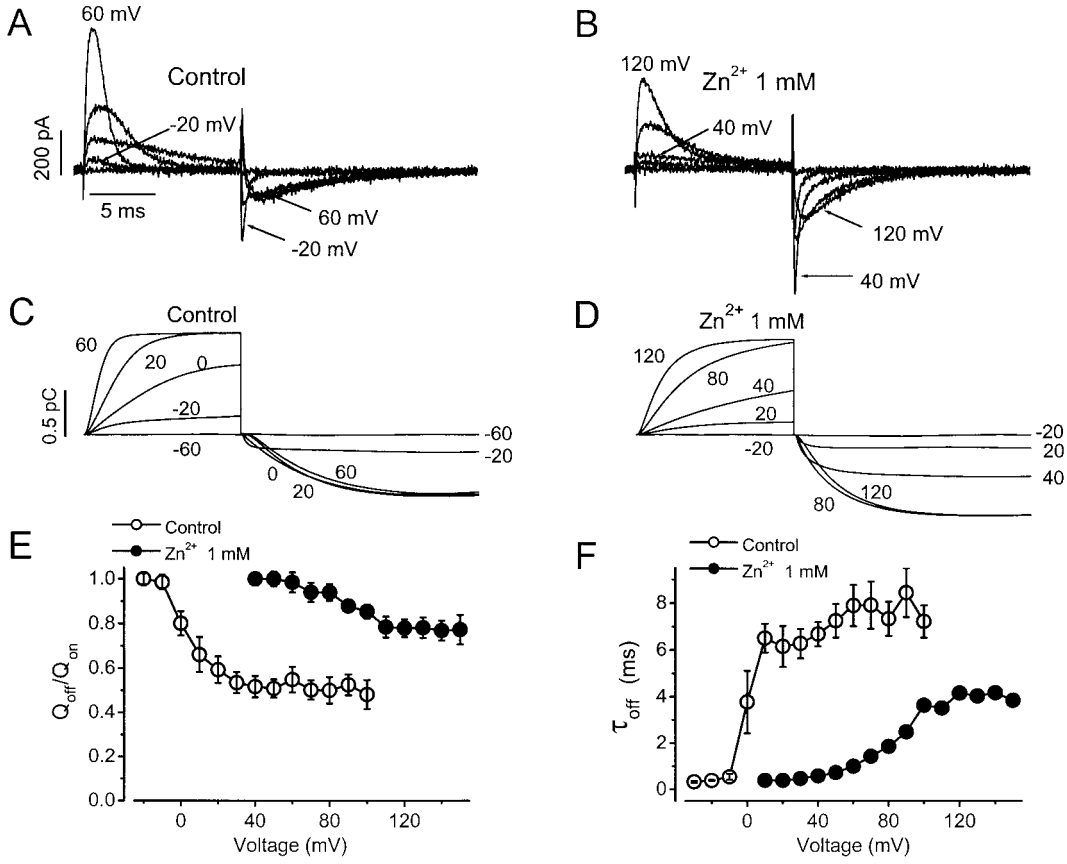

FIGURE 9 External Zn^{2+} speeds gating charge return in Kv1.5 channels. (*A* and *B*) Gating currents evoked from the holding potential of −100 mV in the absence (*A*) and presence (*B*) of 1 mM Zn^{2+}. Pulses were for 12 ms to −60, −20, 0, +20, and +60 mV in the control solution (*A*) and to −20, +20, +40, +80, and +120 mV in 1 mM Zn^{2+} (*B*). (*C* and *D*) Q_{on} and Q_{off} obtained by integration of gating currents in *A* and *B*. (*E*) Mean ratios of Q_{off}/Q_{on} as a function of the step potential in control (○) and 1 mM Zn^{2+} (●). (*F*) Time constants of single exponential fits to the off-gating currents at −100 mV (τ_{off}) as a function of step potential in control (○) and in Zn^{2+} (●). Data in *E* and *F* are the average of six cells.

state. As expected from our knowledge that channel activation is slowed in the presence of Zn^{2+}, the charge movement during activation is also slowed (Fig. 9 *D*). In control conditions (Fig. 9 *C*), the time course of off-charge (Q_{off}) movement is clearly slowed compared with on-charge (Q_{on}) movement. The charge return was so slow that not all charge had returned during the 18-ms period of integration. As a result, the ratio of charge (Q_{off}/Q_{on}) is ~0.5 in control conditions (Fig. 9 *E*). The slowing of off-gating charge return was reduced by 1 mM Zn^{2+} (Fig. 9, *B* and *D*), and this can be clearly seen in the rapid rising phase of the charge records on repolarization. The net effect of Zn^{2+} was to allow more charge return during the integration period, and thus Q_{off}/Q_{on} was ~0.8 (Fig. 9 *E*). We also compared the time course of the off-gating current decay in the absence and presence of Zn^{2+} from data in Fig. 9, *A* and *B*. The time course of off-gating current decay is fit quite well by a mono-exponential function, and in Fig. 9 *F* decay time constants (τ_{off}) of the off-gating currents are plotted versus depolarization voltages. Zn^{2+} significantly reduced τ_{off} at all voltages tested.

DISCUSSION

Prominent action of Zn^{2+} on Kv1.5 gating

In the present study, we have demonstrated that external Zn^{2+} has a significant effect on the gating currents of Kv1.5 channels. Zn^{2+} affects on-gating charge movement by shifting the potentials at which charge is moved to more positive values and also reduces the voltage sensitivity of channel gating, which results in a decreased slope of the charge-voltage (*Q-V*) relation. Higher concentrations of Zn^{2+} also reduce the maximum amount of charge moved. In contrast to the large effects on on-gating charge, off-gating charge is mildly accelerated in the presence of Zn^{2+}. Part of the Zn^{2+} action on gating currents can be attributed to Zn^{2+} binding to the channels and causing a gating shift, and the remaining effect of Zn^{2+} to shift the voltage dependence of charge movement is coupled to the blocking action of Zn^{2+}. Interventions that reduce this blocking action can reduce the shift of the *Q-V* relation in Zn^{2+}.

These gating current observations are consistent with known ionic current actions of Zn^{2+} reported previously in squid axon and *Shaker* K^+ channels (Gilly and Armstrong, 1982a; Spires and Begenisich, 1992, 1994), and on Kv1.5 channels (Harrison et al., 1993; Zhang et al., 2001). Zn^{2+} is known to affect the channel activation kinetics much more than deactivation kinetics (Gilly and Armstrong, 1982a), and this effect is also illustrated in the first figure of the present paper (Fig. 1 *F*). Channel activation is markedly slowed, whereas deactivation is little changed (Spires and Begenisich, 1994) or even accelerated somewhat (Fig. 1 *F*) (Gilly and Armstrong, 1982a). This kinetic shift results in a movement of the conductance-voltage relation tens of millivolts to the right along the potential axis at low millimolar Zn^{2+} concentrations (Fig. 1 *E*). In addition, Zn^{2+} has a variable potency blocking action in different channels including Kv1.5 (Poling et al., 1996; Zhang et al., 2001). Due to the differential effects on activation and deactivation, a general surface charge screening is not likely to account for the Zn^{2+}-induced gating shift, and Gilly and Armstrong (1982a,b) were the first to suggest specific binding to the voltage sensor region of squid axon Na^+ and K^+ channels. Raising the external K^+ or Cs^+ concentration relieves the Zn^{2+}-induced reduction of Kv1.5 ionic current but has no effect on the Zn^{2+}-induced *g-V* shift, so we have suggested that the blocking actions and gating shift induced by Zn^{2+} are mechanistically distinct (Zhang et al., 2001).

Zn^{2+} effects on the *Q-V* relation are potential independent

The over-expression of Kv1.5 channels in mammalian cells allows the recording of K^+ channel gating currents uncontaminated by other current components. This experimental system has allowed us to make novel observations on the actions of Zn^{2+} on Kv1.5 gating systems. Zn^{2+} produces a +55-mV shift of the *Q-V* relation to the right along the potential axis (Fig. 2 and Table 1), and this is accompanied by a significant decrease in slope. Strikingly, this *Q-V* shift significantly exceeds the *g-V* shift induced by Zn^{2+} (Fig. 2 *E*). It is known that K^+ channel gating currents can be segregated into two sequentially coupled charge systems in both *Shaker* and Kv1.5 channels (Bezanilla et al., 1994; Hesketh and Fedida, 1999), and here we have observed that Zn^{2+} apparently affects both charge systems equally (Figs. 2 *C* and 3). From data in Fig. 2 *C* it was apparent that the voltage dependence of both the Q1 and Q2 components was right-shifted by a similar amount along the potential axis, and there was a comparable decrease in the voltage sensitivity (increase of slope factor) of both components (Table 1). Experiments in Figs. 3 and 4 showed that an action on Q2 alone was observed, whether or not Q1 had previously been moved. This suggested that Zn^{2+} was able to bind or remain bound to multiple channel states within the activation pathway. During these experiments it was also noted that the actions on Q1 and Q2 were fully developed as soon as channels were depolarized in the presence of Zn^{2+} (Figs. 2 *B*, 3, and 4), and this suggests unfettered access of Zn^{2+} to closed channels, as was suggested in a study of Zn^{2+} modulation of neuronal A current (Kuo and Chen, 1999).

Not only was there a shift in the voltage-dependent kinetics of the on- and off-gating charge movement, but there was also a 10–15% reduction of the total charge moved at 1 mM Zn^{2+} in 0 mM external K^+ (Fig. 2 and Table 1). These conditions are associated with >90% reduction of ionic current (Fig. 6) and suggests that the blocking action of Zn^{2+} is associated with a prevention of very late transitions in the activation pathway, perhaps in the final con-

certed rearrangements associated with channel opening. Of interest is that ~10% of total charge movement is now thought to be associated with these very last steps to opening (Schoppa and Sigworth, 1998; Ledwell and Aldrich, 1999), which is consistent with the level of charge reduction that we have observed under conditions that prevent almost all ionic current. When external Cs^+ was present at 135 mM (Fig. 7) and block was greatly reduced (Fig. 8), this effect on total charge movement was lost. This action of Zn^{2+} to reduce Q_{max} points to an allosteric mechanism of channel block, rather than (or in addition to) a direct prevention of ion permeation through an open pore (Zhang et al., 2001). Such a mechanism is also supported by the surprising observation we have made here, which is that the blocking action of Zn^{2+} itself is correlated with some gating shift. This is discussed further below.

The slowing of on-gating currents in the present experiments is somewhat reminiscent of the effects of Zn^{2+} on gating currents reported by Gilly and Armstrong (1982b) from Na^+ channels. They noted decreased peak currents and an overall slowing of on-gating current over a wide range of potentials, but these were accompanied by only a +6-mV shift in the *Q-V* distribution, which was comparable with the +8.4-mV shift of the g_{Na}-*V* curve. Overall, the maximum Na^+ channel gating charge moved (Q_{max}) was relatively unaffected by Zn^{2+}, as were the off-gating currents, although in comparison, the Na^+ channel g_{max} was reduced by 30%. In contrast to these results, Spires and Begenisich (1995) found, in squid axon K^+ channels, that large changes in ionic current activation kinetics caused by Zn^{2+} were accompanied by minor slowing of gating currents only near −30 mV, although again there was little change in the total charge movement. As a result they concluded that Zn^{2+} interacts with channel components involved in weakly voltage-dependent conformational changes (Spires and Begenisich, 1995). It is apparent from these studies that different channels vary in their sensitivity to Zn^{2+} and that Kv1.5 channels are among the more sensitive. Not only was the potential shift of the *Q-V* relation very large in Kv1.5 channels, but also there was a significant decrease in the voltage sensitivity of charge movement as shown by the increase in slope factor from 5.9 to 13.1 mV and a reduction in Q_{max} by 13% (Fig. 2 *C* and Table 1).

Zn^{2+} accelerates charge return

In voltage-gated K^+ channels the potential dependence of gating charge return after depolarization is bimodal. It was seen in Fig. 2 that after small depolarizations to −20 mV, charge return is fast, like outward charge movement. However, in the absence of permeating ions, on repolarization after channel opening there is a rising phase to off-gating currents and slowed decay, as illustrated by the off-gating current records at −100 mV on repolarization from +80 mV (Perozo et al., 1993; Stefani et al., 1994). Much of this slowing is due to the relative voltage independence of the last closed-open transition and the concerted rearrangement of subunits in the final steps to opening (Zagotta and Aldrich, 1990; Zagotta et al., 1994; Ledwell and Aldrich, 1999). Our initial experiments revealed that Zn^{2+} was able to speed the return of off-gating currents (Fig. 2 *B*), and this was confirmed by the more detailed analysis in Fig. 9. Zn^{2+} effectively halved the time constant of decay of off-gating currents, and here, as in the *Q-V* relation, a diminished voltage sensitivity of the system was apparent in the presence of Zn^{2+} (Fig. 9 *F*). At least three interventions are known to accelerate charge return in K^+ channels. 4-Aminopyridine (4-AP) accelerates the time course of *Shaker* and Kv1.5 channel off-gating currents (McCormack et al., 1994; Bouchard and Fedida, 1995), and this has been interpreted as a prevention of the late slow steps in channel activation gating that lead to opening. In *Shaker* K^+ channels, external Ba^{2+} speeds off-gating current and accelerates the return of gating charge upon repolarization (Hurst et al., 1997) reflecting Ba^{2+} destabilization of the open channel conformation. Monovalent cations also speed off-gating current and return of gating charge (Chen et al., 1997; Starkus et al., 1998). In the present experiments the results could reflect both Zn^{2+} destabilization of the open state, which can account for the ionic tail current acceleration described in Fig. 1 *F*, and also prevention of late gating steps to opening, which reduces the total charge moved under these conditions (Table 1). This action of Zn^{2+} on off-gating charge is relatively small compared with, for example, the action of 4-AP and may explain the small and sometimes variable action on K^+ channel tail currents (Gilly and Armstrong, 1982a).

A larger voltage-dependent shift of the *Q-V* than of the *g-V* relation

In Kv1.5, Zn^{2+} induced a shift of the *Q-V* curve that was significantly greater than that seen with the *g-V* curve (Fig. 2 *E*). Furthermore, in conditions where the blocking effect was mostly relieved by increasing the concentration of external monovalent cations (Figs. 6 and 8), Zn^{2+} caused a comparable shift of the *Q-V* and *g-V* relations. These results suggest that in addition to the gating-shift site, binding of Zn^{2+} at the blocking site contributes to the *Q-V* shift. In ionic current recordings, channels with Zn^{2+} bound to the blocking site do not conduct, so that the gating shift associated with Zn^{2+} binding at this site is invisible when the *g-V* relationship is measured (Zhang et al., 2001). Therefore, only binding to the site that modulates the gating shift contributes to the *g-V* shift in ionic current recording. In short, the ~2-fold greater shift of the *Q-V* relation compared with the *g-V* relation suggests that binding both to the gate-shifting site and blocking site occur when the channel is closed, and both contribute to the *Q-V* shift.

A strong linear relationship between the shift in gating (*g-V*) and the block caused by Ca^{2+} in Na^+ channels has been used to suggest that a single binding site may be responsible for both actions of the divalent cation in the GH3 pituitary cell line (Armstrong and Cota, 1991), although such a single binding site in Na^+ channels has been questioned for both Ca^{2+} and Zn^{2+}, based on a study of wild-type and mutant rat skeletal muscle Na^+ channels (Sun et al., 1996). Still, in Kv1.5 the observation that current reduction is also closely associated with a gating shift led us to examine the nature of the relationship between block and the overall shift in gating caused by Zn^{2+}. We concentrated on the *Q-V* shift as this relationship measures gating elements from all channels, not just those that are able to open as reported by any *g-V* shift. In Fig. 10, the relationship between the *Q-V* shift and the current reduction are shown at two different K^+ concentrations. It can be seen that at 0 mM external K^+ the reduction of g_{max} is almost linearly related to the ability of Zn^{2+} to shift the *Q-V* relationship. This reflects the small difference between the K_D values for Zn^{2+} actions at the blocking site and the gate-shifting sites (69 vs. 140 μM, respectively) observed experimentally. An increase in external K^+ to 5 mM alters the relation in a manner that is not consistent with a single Zn^{2+} binding site but that can be explained using a two-site binding model simply by an increase in the K_D for the blocking site to 595 μM. The mechanisms by which Zn^{2+} induces a gating shift by actions at the two sites are not known. A simple explanation is that the binding of positively charged Zn^{2+} ions to the external side of the channel changes the voltage field sensed by the voltage sensor so that the closed state is stabilized and large depolarizations are required to open the channel.

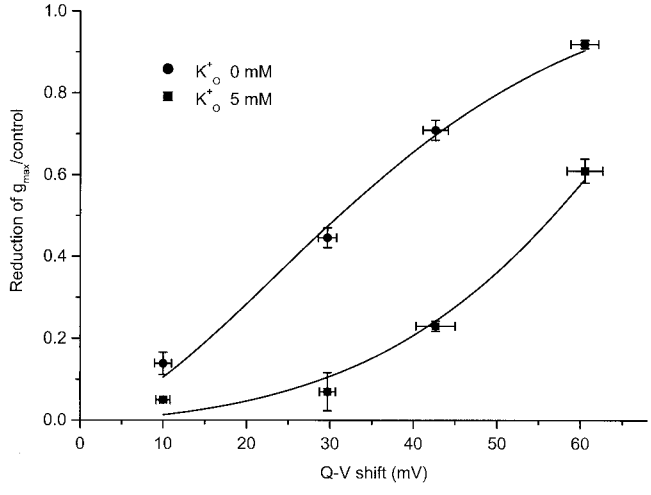

FIGURE 10 Relationship between Zn^{2+}-induced ionic current reduction and the *Q-V* shift. The fraction of the block of outward Kv1.5 current is plotted as a function of the shift of the mid-point of the *Q-V* relation in external solution containing 0 (●) or 5 mM K^+ (■). The solid lines represent the fits assuming that the current reduction and the *Q-V* shift reflect binding to separate sites that can each be described by Hill equations with independent K_D values. At 0 mM K^+_o, a K_D for Zn^{2+} block of 69 μM from Zhang et al. (2001) was used to fit the data, and a K_D for the *Q-V* shift of 147 μM was obtained. At 5 mM K^+_o the K_D for the *Q-V* shift of 147 μM was used to fit data and obtain a K_D for block of 595 μM, which is in close agreement with the experimentally obtained value of 650 μM.

Our observation that the conductance decrease mediated by Zn^{2+} is not voltage dependent (Zhang et al., 2001) implies that the binding site involved in the current reduction and part of the gating shift is located in the outer pore mouth. This, coupled with the well-known ability of Zn^{2+} to bind to His residues, points to Kv1.5 H463 in the channel turret, as defined by the homology with the KcsA channel (Doyle et al., 1998), as a putative binding site. Some support for this hypothesis comes from mutational studies that have shown the equivalent residue (H452) plays a role in proton block of rat Kv1.5 currents (Steidl and Yool, 1999) and from unpublished data we have obtained suggesting that Zn^{2+} and H^+ act via a common site to block Kv1.5 currents. It is known that there are electrostatic interactions between residues in S4 and S6 that affect conformational changes of the pore (Loots and Isacoff, 2000) so there is the possibility that the binding of Zn^{2+} to (or the protonation of) H463 could exert an electrostatic effect on the gating apparatus. As to the site that exerts most of the gating shift, we have no information to identify its location though it is presumably close to the gating assemblies (S2 and S4).

State-dependent binding of Zn^{2+}?

Based on the fact that Zn^{2+} affected activation of K^+ channels in squid axons much more than deactivation, it has been proposed that Zn^{2+} dissociates from squid axon K^+ channels during the transition to the open state (Gilly and Armstrong, 1982a). In rat neurons, Zn^{2+} was reported to bind selectively to closed and deactivated channels (Kuo and Chen, 1999). Both of these models suggest state-dependent binding of Zn^{2+} to K^+ channels. Our results complicate interpretations of this kind because the kinetic data indicate the presence of more than one binding site on the Kv1.5 channel. The *Q-V* data (Fig. 2 and Table 1) unequivocally demonstrate Zn^{2+} binding to multiple states within the activation pathway, including closed states. This results in the large gating shift both of the *Q-V* and the *g-V* and reduced voltage sensitivity (Figs. 1 and 2). Deactivation is faster in the presence of Zn^{2+}, and off-gating charge return is accelerated (Fig. 9). This suggests Zn^{2+} bound to channels as they close, but it is not clear whether this is Zn^{2+} bound to the site that shifts gating or the site that mediates current reduction. Clearly, from Figs. 5–8 the blocking action of Zn^{2+}, which is partially relieved by increased $[K^+]_o$ or $[Cs^+]_o$, is also partly responsible for the shift of the *Q-V* relation. We found that although changing external $[K^+]$ modulated Zn^{2+}-induced slowing of activation (Zhang et al., 2001), it does not affect the deactivation rate (data not shown). This is consistent with the idea that blocking site

binding is reduced on channel opening and residual binding to that site, and the site that shifts gating results in the acceleration of deactivation. In this case, binding to the site that predominantly mediates the shift of gating is not necessarily state dependent.

CONCLUSION

Zn^{2+} reduced the maximum conductance and greatly slowed activation of Kv1.5 currents with a moderate acceleration of deactivation. Zn^{2+} caused an almost twofold greater depolarizing shift of the *Q-V* than of the *g-V* relation and also reduced Q_{max}, and these actions were caused by binding to closed states within the activation pathway. Relief of Zn^{2+} block by K_o^+ or Cs_o^+ also partly relieved the Zn^{2+}-induced *Q-V* shift such that in conditions where the current reduction was minimized, Zn^{2+} caused a comparable shift of the *Q-V* and *g-V* relations.

We conclude that there are two independent binding sites involved in the Zn^{2+} effects. Whereas binding to one site accounts for current reduction, and binding to the other site accounts for the *g-V* shift seen in ionic current recordings, binding to both sites contributes to the Zn^{2+}-induced shift of the *Q-V* relationship.

We thank Qin Wang for assistance in preparing the cells.

Supported by grants from the Heart and Stroke Foundations of British Columbia and Yukon and the CIHR to D.F. and by a grant from the Natural Sciences and Engineering Council of Canada (NSERC) to S.J.K. S.Z. was supported by a Heart and Stroke Foundation of Canada Research Fellowship.

REFERENCES

Armstrong, C. M., and G. Cota. 1991. Calcium ions as a cofactor in Na channel gating. *Proc. Natl. Acad. Sci. U.S.A.* 88:6528–6531.

Bezanilla, F., E. Perozo, and E. Stefani. 1994. Gating of *Shaker* K^+ channels. II. The components of gating currents and a model of channel activation. *Biophys. J.* 66:1011–1021.

Bouchard, R. A., and D. Fedida. 1995. Closed and open state binding of 4-aminopyridine to the cloned human potassium channel Kv1.5. *J. Pharmacol. Exp. Ther.* 275:864–876.

Chen, F. S. P., D. Steele, and D. Fedida. 1997. Allosteric effects of permeating cations on gating currents during K^+ channel deactivation. *J. Gen. Physiol.* 110:87–100.

Davidson, J.-L., and S. J. Kehl. 1995. Changes of activation and inactivation gating of the transient potassium current of rat pituitary melanotrophs caused by micromolar Cd^{2+} and Zn^{2+}. *Can. J. Physiol. Pharmacol.* 73:36–42.

Doyle, D. A., J. M. Cabral, R. A. Pfuetzner, A. L. Kuo, J. M. Gulbis, S. L. Cohen, B. T. Chait, and R. MacKinnon. 1998. The structure of the potassium channel: molecular basis of K^+ conduction and selectivity. *Science.* 280:69–77.

Elinder, F., M. Madeja, and P. Arhem. 1996. Surface charges of K channels. Effects of strontium on five cloned channels expressed in *Xenopus* oocytes. *J. Gen. Physiol.* 108:325–332.

Frankenhaeuser, B., and A. L. Hodgkin. 1957. The action of calcium on the electrical properties of squid axons. *J. Physiol. (Lond.).* 137:218–244.

Gilly, W. F., and C. M. Armstrong. 1982a. Divalent cations and the activation kinetics of potassium channels in squid giant axons. *J. Gen. Physiol.* 79:965–996.

Gilly, W. F., and C. M. Armstrong. 1982b. Slowing of sodium channel opening kinetics in squid axon by extracellular zinc. *J. Gen. Physiol.* 79:935–964.

Harrison, N. L., H. K. Radke, M. M. Tamkun, and D. M. Lovinger. 1993. Modulation of gating of cloned rat and human K^+ channels by micromolar Zn^{2+}. *Mol. Pharmacol.* 43:482–486.

Hesketh, J. C., and D. Fedida. 1999. Sequential gating in the human heart K^+ channel, Kv1.5, incorporates Q1 and Q2 charge components. *Am. J. Physiol.* 274:H1956–H1966.

Hille, B. 1992. Ionic Channels of Excitable Membranes. Sinauer, Sunderland, MA.

Hurst, R. S., M. J. Roux, L. Toro, and E. Stefani. 1997. External barium influences the gating charge movement of *Shaker* potassium channels. *Biophys. J.* 72:77–84.

Kuo, C. C., and F. P. Chen. 1999. Zn^{2+} modulation of neuronal transient K^+ current: fast and selective binding to the deactivated channels. *Biophys. J.* 77:2552–2562.

Ledwell, J. L., and R. W. Aldrich. 1999. Mutations in the S4 region isolate the final voltage-dependent cooperative step in potassium channel activation. *J. Gen. Physiol.* 113:389–414.

Loots, E., and E. Y. Isacoff. 2000. Molecular coupling of S4 to a K^+ channel's slow inactivation gate. *J. Gen. Physiol.* 116:623–635.

McCormack, K., W. J. Joiner, and S. H. Heinemann. 1994. A characterization of the activating structural rearrangements in voltage-dependent *Shaker* K^+ channels. *Neuron.* 12:301–315.

Perozo, E., R. MacKinnon, F. Bezanilla, and E. Stefani. 1993. Gating currents from a non-conducting mutant reveal open-closed conformation in *Shaker* K^+ channels. *Neuron.* 11:353–358.

Poling, J. S., S. Vicini, M. A. Rogawski, and N. Salem, Jr. 1996. Docosahexanoic acid block of neuronal voltage-gated K^+ channels: subunit selective antagonism by zinc. *Neuropharmacology.* 35:969–982.

Schoppa, N. E., and F. J. Sigworth. 1998. Activation of *Shaker* potassium channels. II. Kinetics of the V2 mutant channel. *J. Gen. Physiol.* 111: 295–311.

Spires, S., and T. Begenisich. 1990. Modification of potassium channel kinetics by amino group reagents. *J. Gen. Physiol.* 99:109–129.

Spires, S., and T. Begenisich. 1992. Chemical properties of the divalent cation binding site on potassium channels. *J. Gen. Physiol.* 100: 181–193.

Spires, S., and T. Begenisich. 1994. Modulation of potassium channel gating by external divalent cations. *J. Gen. Physiol.* 104:675–692.

Spires, S., and T. Begenisich. 1995. Voltage-independent gating transitions in squid axon potassium channels. *Biophys. J.* 68:491–500.

Starkus, J. G., L. Kuschel, M. D. Rayner, and S. H. Heinemann. 1998. Macroscopic Na^+ currents in the "nonconducting" *Shaker* potassium channel mutant W434F. *J. Gen. Physiol.* 112:85–93.

Stefani, E., L. Toro, E. Perozo, and F. Bezanilla. 1994. Gating of *Shaker* K^+ channels. I. Ionic and gating currents. *Biophys. J.* 66:996–1010.

Steidl, J. V., and A. J. Yool. 1999. Differential sensitivity of voltage-gated potassium channels Kv1.5 and Kv1.2 to acidic pH and molecular identification of pH sensor. *Mol. Pharmacol.* 55:812–820.

Sun, Y., I. Favre, L. Schild, and E. Moczydlowski. 1996. A minor contribution of divalent cation binding sites in the outer vestibule to the gating shift in the midpoint of Na-channel activation. *Biophys. J.* 70:A318.

Zagotta, W. N., and R. W. Aldrich. 1990. Voltage-dependent gating of *Shaker* A-type potassium channels in *Drosophila* muscle. *J. Gen. Physiol.* 95:29–60.

Zagotta, W. N., T. Hoshi, and R. W. Aldrich. 1994. *Shaker* potassium channel gating. III. Evaluation of kinetic models for activation. *J. Gen. Physiol.* 103:321–362.

Zhang, S., D. C. H. Kwan, D. Fedida, and S. J. Kehl. 2001. External K^+ relieves the block but not the gating shift caused by Zn^{2+} in human Kv1.5 channels. *J. Physiol. (Lond.).* 532:349–358.